J Bioenerg Biomembr (2011) 43:493–505
DOI 10.1007/s10863-011-9380-5

# Mitochondrial bioenergetic profile and responses to metabolic inhibition in human hepatocarcinoma cell lines with distinct differentiation characteristics

**Rossana Domenis · Marina Comelli · Elena Bisetto · Irene Mavelli**

Received: 5 April 2011 / Accepted: 3 August 2011 / Published online: 1 September 2011


**Abstract** The classical view of tumour cell bioenergetics has been recently revised. Then, the definition of the mitochondrial profile is considered of fundamental importance for the development of anti-cancer therapies, but it still needs to be clarified. We investigated two human hepatocellular carcinoma cell lines: the partially differentiated HepG2 and the undifferentiated JHH-6. High resolution respirometry revealed a marked impairment/uncoupling of OXPHOS in JHH-6 compared with HepG2, with the phosphorylation system limiting the capacity for electron transport much more in JHH-6. Blocking glycolysis or mitochondrial ATP synthase we demonstrated that in JHH-6 ATP synthase functions in reverse and consumes glycolytic ATP, thereby sustaining $\Delta\Psi m$. A higher expression level of ATP synthase Inhibitor Factor 1 (IF1), a higher extent of IF1 bound to ATP synthase and a lower ATPase/synthase capacity were documented in JHH-6. Thus, here IF1 appears to down-regulate the reverse mode of ATPsynthase activity, thereby playing a crucial role in controlling energy waste and $\Delta\Psi m$. These results, while confirming the over-expression of IF1 in cancer cells, are the first to indicate an inverse link between cell differentiation status and IF1 (expression level and regulatory function).

R. Domenis · M. Comelli · E. Bisetto · I. Mavelli (✉)
Department of Medical and Biological Sciences,
MATI Centre of Excellence University of Udine,
p.le Kolbe4,
33100 Udine, Italy
e-mail: irene.mavelli@uniud.it

I. Mavelli
INBB Istituto Nazionale Biostrutture e Biosistemi,
v.le Medaglie d'oro,
00136 Rome, Italy

**Keywords** Tumor metabolism · Mitochondria · ATP synthase · Inhibitor Factor 1 · Mitochondrial membrane potential · Human hepatocarcinoma

## Introduction

Of the essential alterations that define the cancer cell phenotype (Hanahan and Weinberg 2000), "metabolic reprogramming", in which tumour cells switch from mitochondrial oxidative phosphorylation (OXPHOS) to glycolysis even in the presence of oxygen (Warburg phenotype), is considered to be a key hallmark (DeBerardinis et al. 2008) as they are highly dependent on aerobic cytoplasmic glycolysis (Shaw 2006). This aberrant phenotype becomes more pronounced with increased tumour malignancy (Simonnet et al. 2002; Cuezva et al. 2002; López-Ríos et al. 2007). In fact, the avidity for glucose represents a strategy that allows tumour cells to survive with limited oxygen and provides them with a mechanism by which they poison their extracellular environment with acid, thus paving the way for invasion and metastasis (Kroemer and Pouyssegur 2008). Thus, cellular bioenergetics has become a central topic of investigation in cancer biology. Indeed, since therapies that target signal transduction pathways have been found to have many side-effects, cancer research is again being directed at targeting the aberrant mechanisms of tumour metabolism with the perspective of potentiating anticancer agents (Ihrlund et al. 2008; Loiseau et al. 2009; Oliva et al. 2010). The field of cancer cell energy metabolism has been expanding rapidly in recent years, raising renewed clinical and biotechnological interest (DeBerardinis et al. 2008; Frezza and Gottlieb 2009; Cuezva et al. 2009). The induction of glycolysis in cancer cells is now known to be a universal feature of cancer; however, the definition of the mitochon-

drial bioenergetic profile still requires clarification and opinions are discordant. In a large variety of tumours, extensive mitochondrial modifications have been described, including: a decrease in biogenesis (Bellance et al. 2009), alterations in the expression levels and functionality of respiratory chain complexes (Putignani et al. 2008), changes in organelle shape and size (Arismendi-Morillo 2009) and the accumulation of mitochondrial DNA mutations that modify the assembly of OXPHOS complexes (Ishikawa et al. 2008). Moreover, several forms of tumour have been recognized to derive ATP also from OXPHOS in striking contrast with Warburg's hypothesis pointing to the existence of high variability in OXPHOS efficiency between different forms of tumour (Zu and Guppy 2004; Moreno-Sanchez et al. 2007). Indeed, tumour cells require mitochondrial functions other than energy production to survive and proliferate and for controlling metabolic fluxes, i.e. intra-mitochondrial metabolic pathways and the maintenance of mitochondrial membrane potential ($\Delta\Psi m$). Hence, the common idea has emerged that mitochondria are not only bystanders, but are somehow involved in the cell transformed state (Frezza and Gottlieb 2009). Pedersen and co-workers have proposed that mitochondria, despite their impaired efficiency, promote and sustain the glycolytic pathway in cancer cells, and they suggest that a biochemical strategy to suppress accelerated tumour proliferation efficiently would be the simultaneous blockade of glycolysis and mitochondria ATP-generating pathways (Mathupala et al. 2010). Indeed, the therapeutic benefits of blocking mitochondrial function in tumour cells, in combination with treatment with glycolytic inhibitors, have also been reported by other authors (Kurtoglu and Lampidis 2009). The correlation between impaired OXPHOS and tumour aggressiveness has been repeatedly reported, as has the fact that altered mitochondrial bioenergetics play an important role in cancer development (Simonnet et al. 2002; Sanchez-Arago et al. 2010). In certain types of carcinoma, a reduced expression of the ATP synthase β subunit was reported to be accompanied by an increased expression of some glycolytic markers (Cuezva et al. 2002). Thus, the level of β-F1ATPase, normalised to mitochondrial mass and correlated with the level of the glycolytic glyceraldehyde-3-phosphate dehydrogenase, has been considered to be a proteomic feature of cancer, defining a "bioenergetic signature" (BEC) of clinical relevance. The BEC index has been proposed to be an indicator of disease progression in different types of cancer patient, as well as a predictive marker of the cellular response to chemotherapy (Cuezva et al. 2002; Hernlund et al. 2009). It has also been demonstrated that aberrant expression levels of β-F1ATPase play a role in colon cancer progression, which requires the selection of cancer cells with a more repressed phenotype (Sanchez-Arago et al. 2010).

Regarding ATP synthase, studies have shown that its natural inhibitor IF1 (Inhibitor Factor 1) is over-expressed in human cancer cells (Green and Grover 2000; Bravo et al. 2004; Sanchez-Cenizo et al. 2010). IF1 is a nuclear encoded protein of 84 amino acids and it arrests the functioning of ATP synthase when $\Delta\Psi m$ drops (Di Pietro et al. 1988). Considering the reduction of β-F1ATPase, an important question is: why is IF1 expression in cancer cells enhanced? One possibility is that IF1 has a structural role and contributes to the preservation of the inner mitochondrial membrane structure since it has been reported to stabilise oligomers of ATP synthase (Campanella et al. 2009), and this, in turn, could determine cristae shapes (Paumard et al. 2002). On the other hand, as highlighted in a recent review by Solaini and colleagues (Solaini et al. 2010), some pioneer studies have prompted interesting speculation about the functional role of IF1 in tumour metabolism and it has been suggested that the excess of IF1 in tumour cells could result in a more efficient blockade of ATP hydrolysis by ATP synthase (i.e. its reverse mode) as compared to that achieved in normal cells (Chernyak et al. 1991; Bravo et al. 2004). Finally, Cuevza and colleagues recently suggested that the over-expression of IF1 in human carcinomas, in addition to the limited expression of the catalytic β subunit and up-regulation of aerobic glycolysis, represents a mechanism by which the overall bioenergetic activity of ATP synthase is restrained. Thus, they propose that IF1 plays a regulatory role in controlling tumour energetic metabolism, supporting its participation as an additional molecular switch used by cancer cells to trigger the induction of aerobic glycolysis, i.e., their Warburg phenotype (Sanchez-Cenizo et al. 2010).

Our studies aim to define the links, if any, between modifications in the expression/function of the OXPHOS system and the proliferation/differentiation characteristics of two human hepatocarcinoma cell lines. In particular, we focus on ATP synthase function, which is one of the confirmed targets of the altered bioenergetic phenotype of carcinomas (Willers and Cuezva 2010) and on the regulatory role of IF1, investigating both the expression and binding of IFI to the enzyme complex. The results provide interesting substance to support the hypothesis that the over-expression of IF1 observed in the more proliferating/less differentiated hepatocarcinoma cell line may actually serve to regulate the reverse hydrolytic activity of ATP synthase, which is associated with a functional impairment of OXPHOS system, and provides a mechanistic explanation to sustain the $\Delta\Psi m$. In fact, the results show that the OXPHOS background (expression and function) is impaired in the JHH-6 cell line, which exhibits a more proliferating/less differentiated phenotype with the phosphorylating system limiting the capacity of the electron transport system markedly more than in the partially differentiated cell line HepG2. Moreover, ATP synthase

functions in reverse, sustaining ΔΨm at the expense of glycolytic ATP. IF1 expression is up-regulated and this higher expression results in a better yield of IF1 productive association with the ATP synthase complex. In accordance, the pharmacological inhibition of glycolysis or ATP synthase differentially affected ΔΨm, ATP flux and respiration in the two cell lines. Their distinct bioenergetic responses to changing environmental conditions reflect inherent differences in mitochondrial background and plasticity.

## Materials and Methods

### Cell types and culture conditions

Two human hepatocellular carcinoma (HCC) cell lines were studied, namely HepG2 and JHH-6, which are respectively assigned to high and low hepatocytic differentiation grades on the basis of their differential capacities to synthesise albumin a know marker of hepatic differentiation (Grassi et al. 2007). Despite almost undetectable levels of albumin production, JHH-6 is able to synthesise ferritin, thus showing a residual hepatic phenotype. The two cell lines were cultured in different media, but in the presence of the same following concentrations of bioenergetic substrates: 11 mM glucose, 1 mM sodium pyruvate, 4 mM glutamine (bioenergetic substrate-containing cultivation medium). HepG2 were cultured in DMEM (Euroclone, Celbio, Devon, UK) and JHH-6 in William's Medium E (Sigma-Aldrich, St Louis, MO). Both media contained 10% FBS, 100 U/ml penicillin and 100 μg/ml streptomycin. Cells were routinely cultured and used for experiments when approaching 90% confluence. Cell proliferation was evaluated daily for 8 days. The mitochondrial fractions from HepG2 and JHH-6 cell cultures were prepared as previously described (Contessi et al. 2007). Briefly, collected HepG2 and JHH-6 cells were suspended at a concentration of $2\times10^7$ cells/ml in mitochondrial isolation buffer (250 mM sucrose, 1 mg/ml BSA and 2 mM EDTA pH 7.4 plus protease inhibitors cocktail) and sonicated at ice-cold temperature (three 5 s sonications, separated by 30 s intervals). The resultant homogenate was subjected to conventional differential centrifugation: 800xg and 16000xg for 20 min at 4 °C. The final pellet (i.e. crude mitochondria fractions) was resuspended in buffer solution containing 250 mM sucrose, 10 mM Tris–HCl and 0.1 mM EGTA pH 7.4, then used immediately for enzymatic analysis or stored at −80 °C for immunoblotting and immunocapture analyses.

### Confocal microscopy

$5\times10^4$ cells were plated in complete medium on glass coverslips and grown overnight. Cells were stained with the mitochondrial marker Mitotracker Red CMXRos (100 nM) (Molecular Probes, Eugene, OR, USA) in complete medium. After staining, cells were fixed in medium containing 3.7% paraformaldehyde and analyzed using a laser scanning confocal microscope equipped with a 488–534 λ Ar laser and a 633 λ He-Ne laser (Leica TCSNT, Leica Mycrosystem, Wetzler, Germany). Fluorescence intensities were quantified using Metamorph TM software (Crisel Instruments, Rome, Italy) by removing all background signals via the "thresholding" technique.

### Polarographic measurement of respiration rates

Oxygen consumption was measured in intact and permeabilized HepG2 and JHH-6 cells using a Oxygraph-2 k high-resolution respirometer (Oroboros instruments; Innsbruck, Austria). Data were expressed as pmol of $O_2$/min/$10^6$ cells and normalized to mitochondrial mass, determined as the level of citrate synthase activity (mU/$10^6$).

Intact non-permeabilized HepG2 and JHH-6 cells were analyzed in their respective bioenergetic substrate-containing cultivation mediums, while digitonin-permeabilised cells were analyzed in a buffer solution containing: 80 mM KCl, 10 mM Tris–HCl, 3 mM $MgCl_2$, 1 mM EDTA and 5 mM $KH_2PO_4$ pH 7.4. Intact cells were resuspended at $1\times10^6$ cells/ml and measurements taken at 37 °C. After recording routine respiration, 2.5 μM oligomycin was added and oligomycin-independent oxygen consumption recorded. Maximum respiration was achieved by adding 2.5 μM p-trifluoromethoxyphenylhydrazone (FCCP). The optimum FCCP concentration was determined by stepwise titration (0.4–3.2 μM FCCP, data not shown). Non-mitochondrial oxygen consumption was determined using 1 μM Rotenone (which inhibits complex I) and 2.5 μM antimycin A (which inhibits complex III); this was then subtracted from the cell total oxygen consumption rate in order to calculate the mitochondrial respiration rate. The same protocol was used to evaluate mitochondrial adaptation when glycolysis was blocked. Briefly, cells were incubated for 1 h in recording solution (156 mM NaCl, 3 mM KCl, 2 mM $MgSO_4$, 1.25 mM $KH_2PO_4$, 2 mM $CaCl_2$ and 20 mM HEPES, pH 7.4) with 5 mM 2-deoxy-D-glucose (2DG) plus 5 mM pyruvate. Permeabilized cells ($1\times10^6$ cells/ml) were used for measuring the activities of the individual respiratory complexes following the addition of freshly prepared digitonin at a concentration previously determined using the trypan blue test (20 μg/$1\times10^6$ cells for JHH-6 and 3 μg/$1\times10^6$ cells for HepG2). After 10 min of incubation with digitonin, the following respiratory substrates and inhibitors were added into the chamber in the following sequence: 10 mM glutamate + 5 mM malate, 5 mM ADP, 1 μM rotenone, 10 mM succinate, 10 mM malonate, 2 mM glycerol-3-phosphate, 2.5 μM antimycin A, 2 mM ascorbate + 200 μM tetramethyl-p-phenylenediamine (TMPD) and 20 mM sodium azide.

Cytochrome *c* (10 μM) was added in a parallel experiment to test for the intactness of the mitochondrial outer membrane in digitonin-treated cells. Data were digitally recorded using DatLab4 software (Oroboros, Innsbruck, Austria); oxygen flux was calculated as the negative time derivative of oxygen concentration, cO2(t). Before performing the assays, air calibration and background correction were performed according to the manufacturer's protocol. The oxygen level was maintained above 40% air saturation.

### Cytofluorimetric analysis of ΔΨm

Collected cells were incubated in high potassium recording solution (109 mM NaCl, 50 mM KCl, 2 mM $MgSO_4$, 1,25 mM $KH_2P0_4$, 2 mM $CaCl_2$ and 20 mM HEPES pH 7.4) in order to avoid contributions from differences in the plasma membrane potential (Modica-Napolitano and Aprille 2001), plus 5 μg/mL 5,5′,6,6′-tetrachloro-1,1′,3,3′-tetraethyl-benzimidazolyl-carbocyanine iodide (JC-1, Molecular Probes) or 200 nM tetramethyl rhodamine methyl ester (TMRM, Molecular Probes) for 30' at 37 °C. In the latter case, 200 nM cyclosporine A was also required to inhibit dye export from the cell by the multidrug transporter. The ratio of red to green fluorescence intensities (aggregate to monomer) of JC-1 gives an index of the ΔΨm (Cossarizza and Salvioli 2001). ΔΨm was also investigated in the presence of some specific inhibitors: i.e. 20 μM oligomycin or 40 mM 2-DG to inhibit oxidative phosphorylation or glycolysis, respectively. 10 μM of mitochondrial uncoupler (FCCP) was used as positive control to collapse ΔΨm. Fluorescence was analyzed on a FACSscan flow cytometer (Becton Dickinson, San Jose, CA, USA) equipped with a single 488 nm argon laser and data were acquired on a logarithmic scale using Cell Quest and analyzed with WinMDI 2.8 software.

### ATP content measurements

Intracellular ATP content was determined in cell lysates by luciferin–luciferase bioluminescent assay according to the protocol provided with the ATPlite assay kit (PerkinElmer, Boston, MA). Measurements were performed using a microplate luminometer (Modulus II-Turner Biosystems). Adherent cells were incubated for 2 h in recording solution with either 10 mM glucose or 10 mM glucose plus 2.5 μg/ml oligomycin (glycolytic ATP generation) or 5 mM 2-DG plus 5 mM pyruvate (oxidative ATP production) and ATP content was expressed as a percentage with respect to untreated controls taken as 100%.

### Determination of mitochondrial mass

Activity of the mitochondrial matrix enzyme citrate synthase (CS) was assessed in cell homogenates to provide an estimate of mitochondrial mass. CS activity was recorded spectrophotometrically at 412 nm using a Lambda 14 UV/Vis Spectrophotometer (Perkin-Elmer) as previously described (Srere 1969). Briefly, the background rate of CS activity was obtained by adding cells, after sonication in 1 M Tris/HCl (pH 8.1), to 1 mM 5,5′-dithiobis-2-nitrobenzoate (DTNB) and 10 mM acetyl-coenzyme A. The reaction was started by addition of the substrate (10 mM oxaloacetate). Enzyme activities were expressed as mUnits (mmoles/min) per mg of protein. Moreover, we evaluated the yield of the crude mitochondria fractions from the two cell lines, expressed as protein percentage recovery with respect to total cell homogenate protein levels. Crude mitochondrial fractions were also investigated for the presence of possible contaminants (H3acK18 for the nucleus, Hsp70 for the cytoplasm and flottilin for the plasma membrane) by immunoblotting to be sure that the degree of mitochondrial purification was similar for both cell lines (contaminants ranged between 5% and 20%).

### Mitochondrial ATP synthase activity

The maximal ATPase activity ($V_{max}$) of mitochondrial ATP synthase was measured in an ATP-regenerating system at 25 °C (Grover et al. 2004; Comelli et al. 1994). Mitochondrial membranes were obtained by osmotic shock treatment, by incubating in a medium containing 30 mM sucrose, 50 mM Tris/HCl (pH 7.4), 4 mM $MgCl_2$, 50 mM KCl, 2 mM EGTA 2 mM phosphoenolpyruvate, 0.3 mM NADH, 2 μg/ml rotenone, 4 IU of pyruvate kinase and 3 IU of lactate dehydrogenase. The reaction was started by the addition of 2.5 mM ATP and the rate of NADH oxidation, equimolar to ATP hydrolysis, was monitored as the decrease in absorbance at 340 nm. The ATPase activity was assessed in the presence of 30 μM oligomycin or 20 μM resveratrol. Results are reported as IU defined as 1 μmol oxidized NADH/min/mg. To induce the release of the inhibitor protein IF1 from ATP synthase, the mitochondrial membranes were incubated, where indicated, for 30 min at 37 °C in "activated" conditions composed of 125 mM KCl, 2 mM EDTA and 30 mM Tris-$SO_4$ pH 8.

### Western blot analysis in mitochondrial lysates

Western blot analyses were performed as previously described (Contessi et al. 2007) using the following antibodies: mouse monoclonal anti-NDUFA9 subunit of complex I (Abcam), anti-Fp subunit of complex II (Invitrogen), anti-UQCRC2 subunit of complex III (Abcam), anti-COX IV subunit of complex IV (Abcam), anti-IF1 (Mitosciences), anti-Hsp70 (Abcam), anti-H3acK18 (Abcam), anti-Flottilin-1 (Abcam) and rabbit polyclonal anti-β subunit of ATP synthase (kindly provided by Dr. F. Dabbeni-Sala, Department of Pharmacology,

University of Padua, Italy). Densitometric analysis was performed with Quantity One 4.2.1 software (Bio-Rad Hercules, California). A linear relationship was confirmed in each case between increasing band intensities and the quantities of proteins loaded into the gel in order to prove non–saturating conditions. Quantitative data were inferred on the basis of the slope of the straight line and reported as % of HepG2 expression level, taken as 100%.

### ATP synthase immunoprecipitation and inhibitor protein IF1 immunodetection

To extract ATP synthase, frozen mitochondria were rapidly thawed and treated with digitonin (3 g/g) in 50 mM NaCl, 5 mM aminocaproic acid and 30 mM Tris pH 7.4. Samples were centrifuged at 150000xg for 25 min at 4 °C and the supernatants used to immunoprecipitate ATP synthase and IF1 bound to the enzyme, as previously described (Giorgio et al. 2009). Aliquots were incubated overnight under wheel rotation at 4 °C in the presence of anti-complex V monoclonal Ab covalently linked to protein G-Agarose beads (MS501 immunocapture kit from Mitosciences) in a ratio of 20 µl per mg of protein. After gentle centrifugation (500xg for 5 min), the beads were washed twice for 5 min in a solution of 0.05% (w/v) DDM in PBS. Elution was then performed in 2% (w/v) SDS for 15 min, and the collected fractions were subjected to SDS-PAGE.

### Statistical analyses

The results presented correspond to mean values ± standard deviations (SD); Student's t tests were used to test for statistical significance in the differences between means; $p<0.05$ was considered to be statistically significant.

## Results

### Cell morphology, growth characteristics and mitochondrial content of HepG2 and JHH-6 cell lines

The two HCC cell lines investigated exhibited different cell morphologies and cell sizes (Fig. 1a): the undifferentiated cell type (JHH-6) presented a fibroblast-like morphology, while the partially differentiated cell type (HepG2) presented a polygonal shape, more similar to hepatocytes. In accordance with the different cell sizes observed microscopically, measurements of total protein content confirmed that HepG2 cells were smaller (0.32±0.04 mg/$10^6$ cells) than JHH-6 cells (0.44 ±0.04 mg/$10^6$cells). As expected, on the basis on their distinct differentiation grades, the cells exhibited different doubling time: 16±1.2 h for JHH-6 compared with 30.7±0.5 h for HepG2.

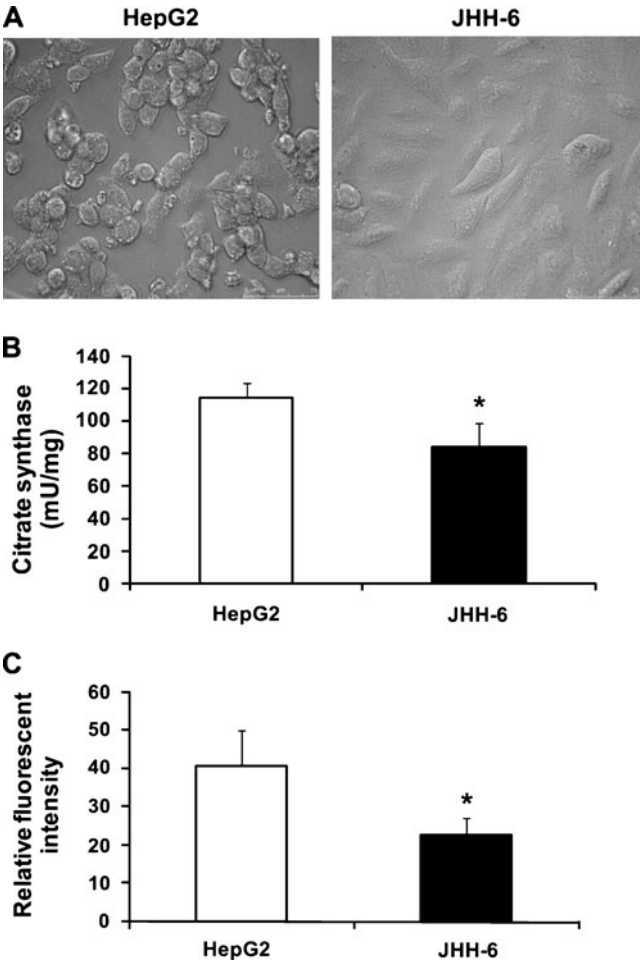


**Fig. 1** Cellular morphology and mitochondrial mass analyses of HepG2 and JHH-6 cells. **a** Cell morphology analyzed by interferential contrast microscopy (Leica AF6000LX Wide Field Microscope, Leica Microsystems, Wetzler, Germany). **b** Enzymatic measurements of CS activity were performed spectrophotometrically on total cell homogenates and activities are expressed as mUnits/mg of total protein; * $p<0.001$ compared with HepG2. Data presented are means ± SD of three independent experiments. **c** Histogram representation of the Mitotracker Red relative fluorescence intensity quantified from confocal images using Metamorph software; * $p<0.001$ compared with HepG2

The mitochondrial yield for the larger, undifferentiated JHH-6 cells was 12%, compared with 21% for the smaller, more differentiated HepG2 cells. For purposes of quality control, crude mitochondrial fractions were analyzed for the presence of cellular contaminants (i.e. the nucleus, cytoplasm or plasma membrane) by immunoblotting using antibodies against specific markers. The contamination levels for these subcellular fractions were similar for both cell lines (data not shown), ruling out the possibility that the difference in mitochondrial yields was due to a difference in contamination levels. Mitochondrial contents were evaluated further by assaying CS activities in total cell homogenates. Due to its location in the mitochondrial matrix, CS is commonly used as a quantitative marker enzyme to evaluate the mitochondrial

content/mass. In accordance with the mitochondrial yield, the results reported in Fig. 1b show that the two cells lines exhibit a significant difference in mitochondrial mass. Mitochondrial mass was further analyzed using Mitotracker Red and visualized by confocal microscopy. The fluorescence intensity of Mitotracker Red, quantified using Metamorph software, was higher in HepG2 than in JHH-6 cells, indicating a higher mitochondrial density in HepG2 (Fig. 1c).

## Oxygen consumption in permeabilised cells: flux control ratios

In order to evaluate the functionality of the different OXPHOS complexes, oxygen consumption in digitonin-permeabilised cells was determined. The amount of digitonin needed for optimal cell permeabilization was experimentally determined for each cell type. Specific substrates and inhibitors were added in sequence to evaluate the activity of the respiratory chain complexes I-IV. Representative respiratory curves of permeabilized cells are shown in Fig. 2a for both cell lines and the corresponding values of oxygen consumption rate are summarized in Table 1 for the single respiratory complexes, expressed as a ratio with respect to the CS activity level. State 3 respiration, assessed in the presence of NADH- and $FADH_2$-dependent substrates, was higher in HepG2 than in JHH-6 cells, while complex IV activity was similar between the two cell lines.

The OXPHOS system is divided into two segments: the oxidative system (OS), formed of substrate transporters, Krebs cycle enzymes and electron transport system (ETS), and the phosphorylating system (PS), consisting of the ATP/ADP (ANT) and Pi (PiT) transporters and ATP synthase. The respiratory control ratio (RCR) for complex I-sustained respiration, i.e. state 3 (ADP excess)/state 4 (ADP limited), was lower in JHH-6, indicating a lower state of coupling between the ETS and the PS (Fig. 2b). The OXPHOS flux control ratio (P/E) relates the OXPHOS capacity (P) (respiration assessed in the presence of glutamate-malate, succinate [convergent CI + II electron supply] and saturating ADP) to the maximal uncoupled respiration (E). P/E represents an index of the ETS's limitations by the PS. A lower P/E was evident in JHH-6 compared with HepG2 cells, indicating that the ETS in the JHH-6 cell line was more restricted by PS (Fig. 2b). Moreover, even when the ETS was fully active, the oxygen consumption (E) was lower in JHH-6, indicating that the ETS *per se* was also working less compared to that of HepG2 (Table 1).

## Metabolic inhibition-mediated modulation of ΔΨm

Although glycolytic ATP synthesis may be sufficient for cell growth, cancer cells need to maintain the integrity of some mitochondrial functions for their survival, and, in particular, to maintain the ΔΨm and mitochondrial homeostasis for $Ca^{2}$+ exchange, ionic transport and the operation of metabolite pathways. ΔΨm was determined in HepG2 and JHH-6 cells using the mitochondrial selective probes TMRM and JC-1. Flow cytometry analyses of each probe showed that ΔΨm was significantly higher in the undifferentiated JHH-6 than in HepG2 cells (Fig. 3a and b).

ΔΨm was also examined following the inhibition of either OXPHOS activity by oligomycin, that selectively blocks ATP synthase, or glycolysis by 2-DG, as well as after treatment with the uncoupler FCCP to cause ΔΨm collapse. Figure 3c shows data from TMRM fluorescence analysis. Data are expressed as percentages of fluorescence intensity *vs.* untreated cells. The reduction of TMRM fluorescence observed in the presence of FCCP was considered as corresponding to complete ΔΨm collapse and was decreased by about 50% in both HepG2 and JHH-6 (not shown). Incubation with oligomycin increased ΔΨm in HepG2, indicating that the $H^{+}$ flux into the mitochondrial matrix was blocked. Conversely, in JHH-6 cells, oligomycin caused ΔΨm to collapse, suggesting that ATP synthase was functioning in reverse in these cells as an ATP hydrolase in order to sustain ΔΨm. On the other hand, inhibition of glycolysis with 2-DG also decreased ΔΨm in JHH-6, indicating that glycolysis and glycolytically generated ATP was required. In contrast, 2-DG increased ΔΨm in HepG2, suggesting an adaptive response of these mitochondria, which were able to increase their activities following the blockade of glycolysis. These results suggest that the maintenance of ΔΨm requires OXPHOS activity in HepG2 and the hydrolysis of glycolytic ATP by ATP synthase in JHH-6.

## Metabolic inhibition-mediated modulation of ATP content

The steady-state of cellular ATP content produced by glycolysis and mitochondrial oxidative metabolism was evaluated in HepG2 and JHH-6 cells using a luciferin/luciferase assay. The effects of different substrates and metabolic inhibitors on the ATP content are reported in Fig. 4a. Under glycolytic conditions (i.e. in the presence of glucose as the lone substrate and oligomycin), a significant reduction of ATP content was observed in HepG2, suggesting a contribution of OXPHOS activity in these cells under routine basal culture conditions. This was in accordance with the increase of ΔΨm caused by oligomycin as well as with the apparent adaptive response of the mitochondria in the presence of 2-DG. Conversely, in JHH-6 ATP was unaffected by glycolytic conditions, suggesting that glycolysis was able to compensate for the impairment of OXPHOS activity, or that under routine basal culture conditions OXPHOS activity was negligible. However, under oxidative conditions (i.e. in presence of pyruvate

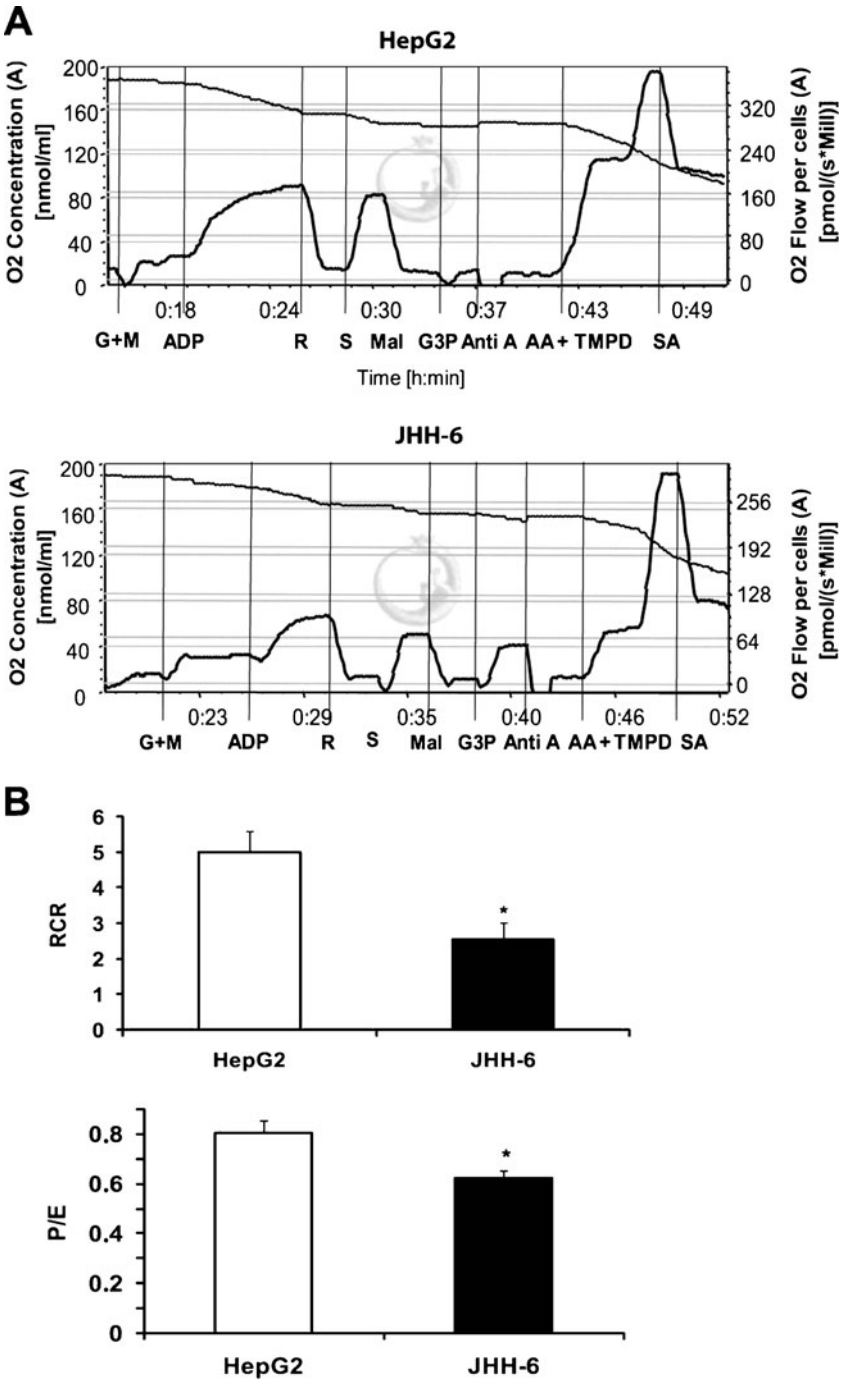


**Fig. 2** Oxygen consumption and flux control ratios in digitonin-permeabilized cells. **a** Representative recordings of oxygen concentration [nmol/ml] (*thin line*) and oxygen flow [pmol/(s*Mill)] (*thick line*) of permeabilized HepG2 and JHH-6 cells measured by high-resolution respirometry in the presence of saturating ADP (state 3 respiration). The following respiratory substrates and inhibitors were added in the following sequence: G, glutamate; M, malate; R, rotenone; S, succinate; Ma, malonate; G3P, glycerol-3-phosphate; AA, antimycin A; AcA, ascorbate; TMPD, *N,N,N',N'*-tetramethyl-*p*-phenylenediamine dihydrochloride; SA, sodium azide. **b** Flux control ratios, RCR and P/E, in permeabilized HepG2 and JHH-6. RCR was obtained by dividing the rate of $O_2$ consumption in state 3 by the rate in state 4 (glutamate + malate). * $p<$ 0.001, compared with HepG2. P/E was calculated from the values in Table 1; * $p<0.01$ compared with HepG2. Values represent means ± SD of four independent experiments

and 2-DG) ATP levels decreased by 70% in both cell lines, whereas, in light of the data reported above, ATP levels were expected to fall down in the case of JHH-6. Thus, we explain this apparent discrepancy by making the hypothesis that in JHH-6 when glycolysis is inhibited, the OXPHOS activity is able to supply ATP, although in a low extent, thereby reducing the effective decrease in ATP level *vs.* HepG2. Nevertheless, these results suggest that glycolysis produces a large amount of ATP (Warburg effect) in both cases.

## Oxygen consumption in intact cells: respiratory flux control ratios and their modifications by metabolic inhibition

Oxygen consumption was determined by high-resolution respirometry in intact cells suspended in routine basal culture medium, a condition that reflects the in vivo situation. Various bioenergetic parameters were determined that characterize the cellular state of aerobic energy production (Gnaiger 2008). Specifically, oxygen consumption under basal conditions provides a measure of the

**Table 1** Oxygen consumption in digitonin-permeabilized cells

| | $0_2$ consumption [pmol/s*Mill)]/CS | |
|---|---|---|
| | HepG2 | JHH-6 |
| Glutamate/malate | 3.17±0.66 | 2.05±0.31 (*) |
| Succinate | 4.66±0.30 | 1.89±0.46 (*) |
| Ascorbate/TMPD | 6.89±0.72 | 7.18±1.43 |
| OXPHOS (P) | 3.80±0.27 | 2.23±0.16 (*) |
| ETS (E) | 4.76±0.16 | 3.49±0.19 (*) |

Rate of oxygen consumption [pmol/(s*Mill)]/CS was assessed in digitonin-permeabilized cells using a multiple substrate-inhibitor analysis for CI, II, and IV. The OXPHOS capacity (P) was assessed in the presence of glutamate, malate and succinate (convergent CI + II electron supply) and saturating ADP. Uncoupled respiration (E) was achieved by titrating FCCP in a stepwise fashion until maximal uncoupled respiration was established; *$p<0.05$ compared with HepG2. Values are means ± SD of four independent experiments

respiration sustained by the endogenous substrates (R: Routine physiological respiration), which was markedly inhibited when oligomycin was added to prevent ATP synthesis. Non phosphorylating respiration (residual in the presence of oligomycin) represents the fraction that is used to drive the futile circle of proton pumping and proton leak back across the inner mitochondrial membrane (L: Proton leak), while phosphorylating-coupled respiration (inhibited by oligomycin) represents the fraction of respiration used for ATP synthesis (R-L). Oxygen consumption was stimulated and the maximum respiration measured (E: Maximum ETS capacity) when OXPHOS was uncoupled by the addition of FCCP. Respiratory flux control ratios were expressed relative to the maximum ETS capacity E, chosen as the common reference state. The routine physiological respiration rate R relative to E (routine flux control ratio R/E) represents the part of the respiratory capacity used by the cells for basal respiration, and reflects the activation state of respiration according to routine ATP

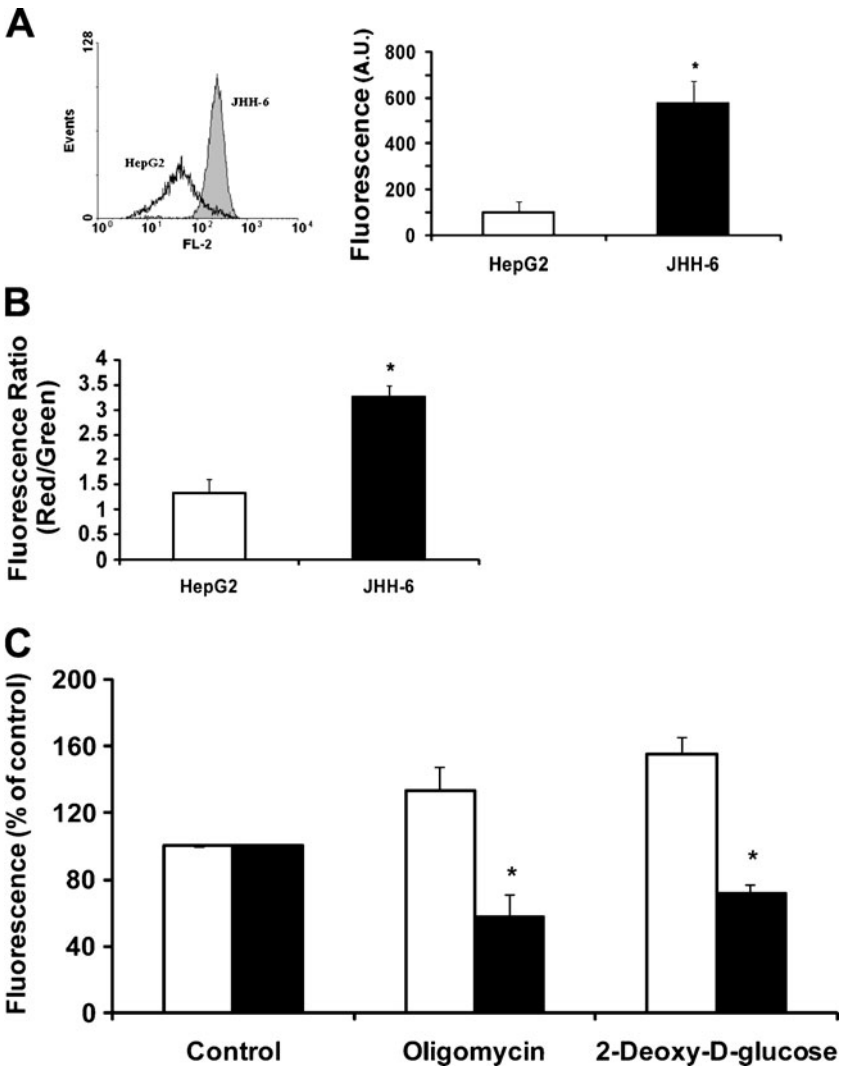


**Fig. 3** Cytofluorimetric analysis of ΔΨm and the effects of metabolic inhibition. **a** HepG2 and JHH-6 cells were stained with 200 nM TMRM. Histogram plot is from one experiment representative of three. Columns represent means ± SD of three independent experiments; * $p<$ 0.005 compared with HepG2. **b** Cells were stained with 5 μg/ml JC-1. The relative values of aggregate/monomer (*red*/*green*) fluorescence intensities were used as an indication of ΔΨm. Columns represent means ± SD of three independent experiments; * $p<0.005$ compared with HepG2. **c** Effect of OXPHOS and glycolysis inhibitors on ΔΨm in HepG2 (*white bar*) and JHH-6 (*black bar*). Cells incubated in recording solution containing 200 nM TMRM were treated with 40 mM 2-DG or 20 μM oligomycin for 30 min at 37 °C. Data are expressed as percentages of fluorescence intensity compared to untreated cells (Control taken as 100%). Values are means ± SD of five independent experiments; * $p<$ 0.005 compared with HepG2

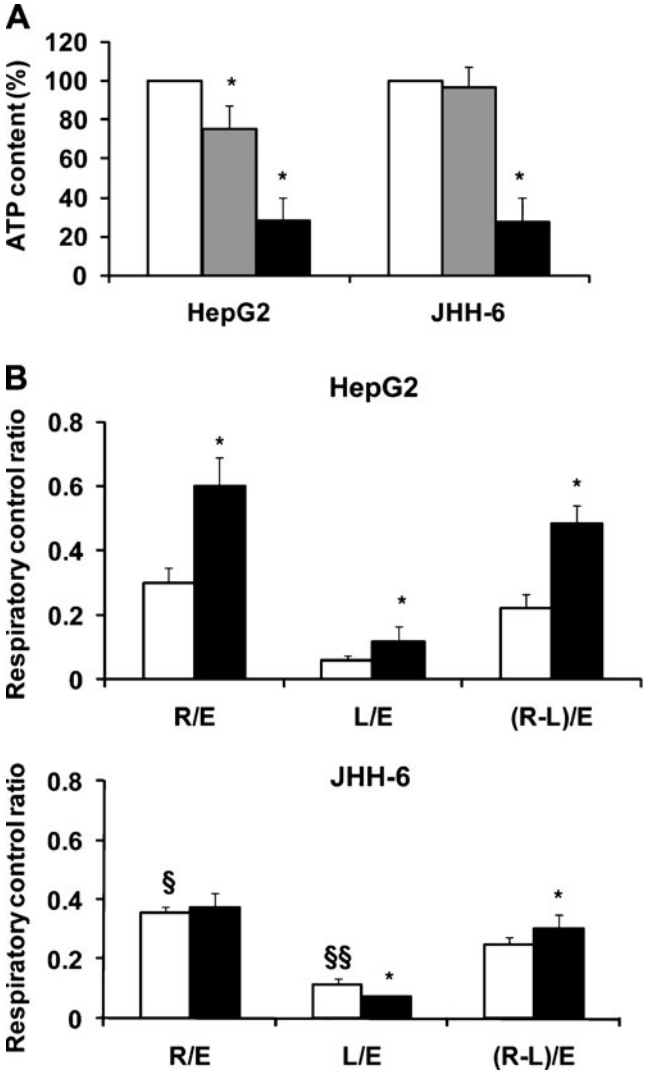


**Fig. 4** Metabolic inhibition-mediated modulation of cellular ATP and oxygen consumption. **a** HepG2 and JHH-6 were incubated for 2 h with either glucose (control cells, *white bar*), or glucose plus oligomycin (glycolytic conditions, *grey bar*), or sodium pyruvate plus 2-DG (oxidative conditions, *black bar*). ATP content was measured in cell lysates using luciferin/luciferase detection. Data are represented as percentages compared with untreated control cells; * $p<0.001$ compared with untreated control cells. **b** Flux control ratios in intact cells. Metabolic states: R = Routine; L = Proton Leak; E = Maximum ETS capacity. R/E = Routine flux control ratio; L/E = Leak flux control ratio; (R-L)/E = Phosphorylating flux control ratio. HepG2 and JHH-6 cells were incubated for 1 h in the presence of 2-DG plus sodium pyruvate (*black bar*) and the effect was compared with the analysis in bioenergetic substrates-containing cultivation medium (*white bar*). Values are means ± SD of six and three independent experiments for control and treatment respectively * $p<0.05$ compared with experiments in culture medium, § $p<0.05$, §§ $p<0.01$ compared with HepG2

demand relative to excess capacity. Correspondingly, the L/E (leak flux control ratio) reflects the level of leak respiration relative to the maximum ETS capacity and provides an estimate of normalized uncoupled respiration. Finally, the fraction of respiration actually used for ATP production (i.e. the normalised phosphorylating respiration) is estimated as (R-L)/E.

L/E ratio is higher in JHH-6 (Fig. 4b), indicating that uncoupling between respiration and phosphorylation was markedly higher than in HepG2. Consequently, the normalized phosphorylating respiration (R-L)/E ratio was lower in JHH-6, i.e. 66% of the R/E ratio, which was considered as 100%; whereas in HepG2, (R-L)/E was 80%. Incubation of HepG2 under oxidative conditions (pyruvate + 2-DG) determined an increase in R/E, as well as a proportional increase in both the L/E and (R-L)/E. This suggests an adaptive activation of silent mitochondria following the blocking of glycolysis. Conversely, in JHH-6 a decrease in L/E was observed after blocking glycolysis with 2-DG, suggesting an optimization of coupling to the PS. No activating adaptive response was observed as indicated by the absence of an effect on the R/E, although an increase in the phosphorylating rate (R-L)/E did occur (Fig. 4b).

## Expression levels of OXPHOS complexes, ATP synthase capacity under physiological and "activated" conditions, and proteomic analysis of the association of the inhibitor protein IF1

The expression levels of the OXPHOS complexes were evaluated by quantitative immunoblot analysis of isolated mitochondria from JHH-6 and HepG2, which were also characterised for cellular contaminants (see above). One representative subunit of each of the five OXPHOS complexes was assayed using a set of antibodies. Results are shown in Fig. 5a, b and c and expressed as % with respect to HepG2. As shown in panels A and B, all the OXPHOS complexes, except for complex III, were significantly lower in JHH-6. The most striking result was obtained for the NDUFA9 subunit of complex I, for which levels were only 18% of those in HepG2. Whereas ATP synthase (complex V) was the complex that showed the least variation in comparison with HepG2 levels, at 63% (Fig. 5c). Immunoblot analysis was also used to measure the expression of the ATP synthase inhibitor protein IF1. IF1 expression was markedly higher (250%) in mitochondria from JHH-6 and apparently in a large excess compared to the expression of the β subunit of ATP synthase (Fig. 5c).

Further functional analyses were performed to evaluate the ATP synthase capacity under physiological and "activated" conditions, and the association of IF1 with ATP synthase in the mitochondrial membrane. The assay to determine the maximal ATP hydrolytic activity of ATP synthase was done on osmotic shock-treated mitochondria. Sensitivity to the selective inhibitors resveratrol or oligomycin was evaluated in order to eliminate the possible contributions of non-mitochondrial contaminant ATPases

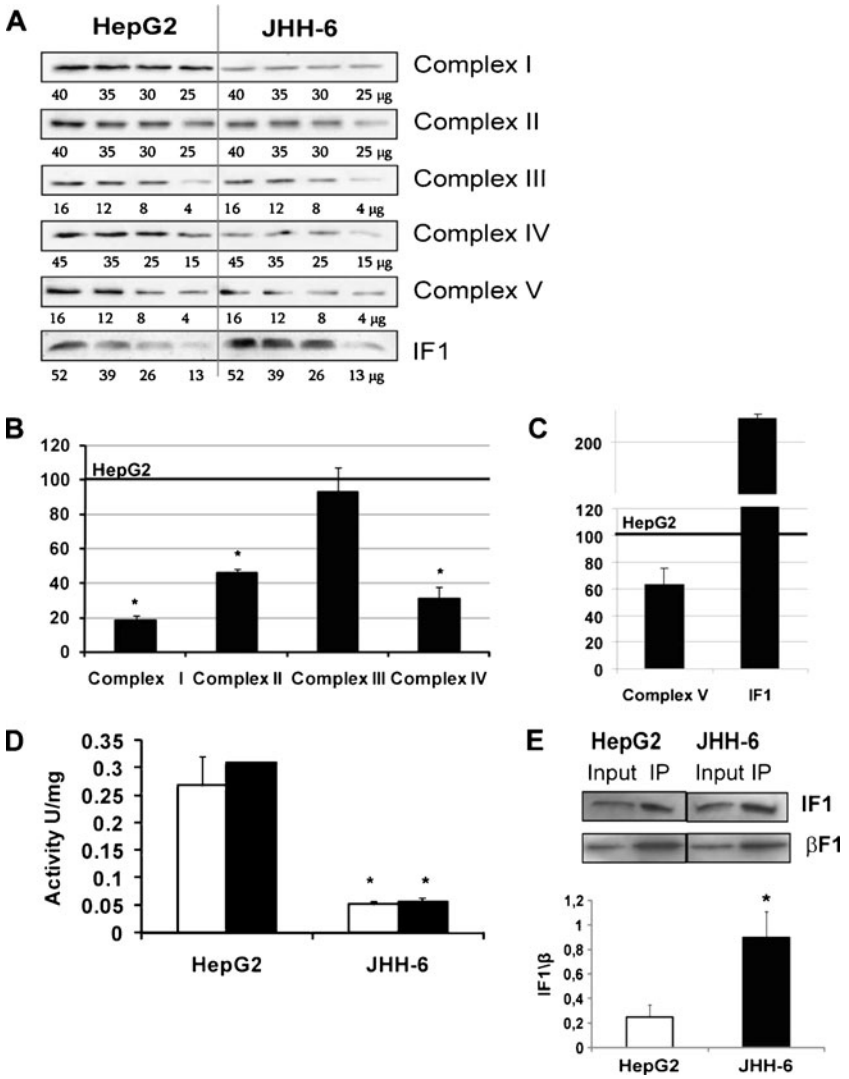


**Fig. 5** Analysis of OXPHOS complex expression levels and ATP synthase activity and regulation by IF1. **a** Western blot analysis of representative subunits of OXPHOS complexes and IF1 was carried out using crude mitochondrial fractions from HepG2 and JHH-6 cells. Different quantities of proteins were separated by SDS/PAGE, trans-blotted and identified with specific antibodies: complex I (NDUFA9), II (Fp), III (UCRQ), IV (COX-IV) and V (β-F1-ATPase), followed by quantitative densitometric analysis. **b-c** OXPHOS complexes and IF1 expression levels in JHH-6 mitochondrial fractions compared with HepG2 levels considered as 100%. Quantitative data were inferred by densitometric analysis of immunoreactive bands. Means ± SD of four independent experiments; * $p<0.05$ values compared with HepG2. **d** ATPase capacity (Vmax) was measured as described in "Materials and Methods". *White bars*: oligomycin-sensitive ATPase activity as a measure of ATP synthase capacity; *Black bars*: resveratrol-sensitive ATPase activity as a measure of the authentic mitochondrial activity. Mean of five different determinations is shown together with the standard deviation; * $p<0.05$ compared with HepG2. **e** Immunocapure analysis of IF1 association with ATP synthase. ATP synthase-enriched mitochondrial digitonin extracts were subjected to immunoprecipitation with anti-complex V antibodies and analyzed for IF1 and for the β subunit of the F1 sector of the complex by immunoblotting. IP: immunoprecipitated fraction; Input: mitochondrial detergent extract used as control. Graphical representation of the ratio IF1/β obtained by densitometric analysis of the immunoreactive bands. Values are means ± SD of three independent experiments * $p<0.01$ compared with HepG2

and to have a measure of only the correctly assembled ATP synthase complex able to synthesize ATP, thereby assaying the ATP synthase capacity of the enzyme (Grover et al. 2004). In fact, while resveratrol targets F1, oligomycin requires the whole ATP synthase complex to be effective. As shown in Fig. 5d, in both HepG2 and JHH-6 cells the oligomycin-sensitive ATPase activity (white columns) was comparable with resveratrol-sensitive ATPase activity (black columns), indicating that the entire enzyme was correctly assembled in each cell line. Activity is significantly lower in JHH-6, corresponding to 25% of that in HepG2. In order to evaluate whether IF1 inhibited the enzyme to different extents in the two cell lines, ATPase activity was measured in "activated" conditions that are able to strip IF1 from the

complex. Considering that alkaline-high salt treatment removes >95% of bound IF1 (Rouslin and Broge 1996), the ATPase activity observed in this condition was taken as the activity of IF1-free enzyme and thus considered as maximal activity (100%). On this basis, we calculated the ratio of control to IF1-free enzyme activities (measured in normal [pH 7] and alkaline-high salt conditions, respectively; CTRL *vs.* IF1-stripped) and used this ratio as a measure of the amount of IF1-inhibited enzyme. HepG2 cells presented 16% of IF1-inhibited enzyme, whereas 32% was IF1-inhibited in JHH-6 (Table 2).

These data are consistent with the hypothesis that ATP synthase activity may be more tightly regulated in JHH-6 than in HepG2 cells due to the higher expression level of IF1 observed in mitochondria from JHH-6. The results of the proteomic analysis carried out to evaluate the association of IF1 with ATP synthase in the mitochondrial membrane also support this hypothesis. Total digitonin-treated mitochondrial extracts were subjected to immunoprecipitation with anti-complex V antibodies and analyzed by SDS-PAGE and immunodetection with antibodies recognizing the β subunit of ATP synthase and IF1. Total digitonin-treated extracts were also analyzed for the two proteins as a control of detergent-extraction. As shown in Fig. 5e, the IF1/β ratio was higher in JHH-6 (IF1/β=0.90±0.21) respect to HepG2 (IF1/β=0.25±0.10). Taken together, these results suggest that mitochondria from JHH-6 have a higher IF1 content and a higher degree of IF1 association with ATP synthase, thus contributing to the negative regulation of the enzyme.

## Discussion

The question of impaired mitochondrial function in cancer cells was first raised almost 50 years ago (Warburg 1956), and although the enhancement of glycolysis in cancer cells has now been well explained, the silencing role of mitochondrial OXPHOS remains poorly understood. Today, cancer research is being redirected towards targeting the aberrant metabolism of tumours.The occurrence of divergent observations raises fundamental questions regarding variability in metabolic reprogramming between cancers and the relative contributions of oncogenesis, tumour environment and proliferative activity upon tumour phenotype. In view of these considerations, it has been suggested that the mitochondrial bioenergetic background of a tumour should be taken into account when personalizing anticancer treatments (Loiseau et al. 2009). In fact, evidence has come to light indicating that the mitochondrial OXPHOS background confers a survival advantage to more differentiated cells which can, as a result, escape chemotherapy by activating their oxidative metabolism (Marroquin et al. 2007). Thus, any parameter defining the mitochondrial bioenergetic profile of a specific tumour cell and that varies as a function of tumour grading and proliferation may represent a useful tool for predicting the prognosis and sensitivity to the distinct therapeutic strategies.

**Table 2** Activation of ATP hydrolysis under conditions of IF1 release

| ATPase activity | HepG2 | JHH-6 |
|---|---|---|
| CTRL | 0.28±0.01 (84%) | 0.044±0.001 (68%) |
| IF1-stripped | 0.33±0.01 (100%)* | 0.065±0.002 (100%)* |

Mitochondria permeabilised by osmotic shock were assayed after incubation for 30 min at 37 °C in alkaline-high salt conditions (IF1-stripped) or in assay buffer (CTRL); oligomycin-sensitive ATPase activity is reported. Means ± SD of three independent experiments; *$p<0.001$ compared with control

In the present study, we first analyzed the OXPHOS system of two HCC cell lines with different growth/differentiation characteristics, in order to deeply investigate if OXPHOS modifications are associated with tumour cell differentiation. We found the OXPHOS system to be more impaired in undifferentiated, JHH-6 cells, which have lost most of the morphological and differentiation characteristics related to the original tissue, whereas the OXPHOS system in HepG2 cells, which retain characteristics of differentiated cells, were less impaired. In JHH-6, lower expression levels of the OXPHOS complexes I, II, IV and V were found compared to HepG2 cells. The activities of the single ETS carriers and RCR were also lower in JHH-6, and a low PS capacity limited the ETS capacity much more that in HepG2. Moreover, ΔΨm was higher in JHH-6 than in HepG2, in accordance with data from other authors that indicate the ΔΨm to be higher in carcinoma cells than in normal epithelial cells (Kurtoglu and Lampidis 2009) and that this increase appears to correlate with features of tumour aggressiveness (Kim et al. 2007). At this time, no real understanding of the biochemical basis for these observations exists, which may include the differences observed in mitochondrial respiratory enzyme complexes, ATP synthase and IF1expression level and regulatory function (discussed below), as well as putative differences in ATP/ADP transport, uncoupling proteins (UCPs) and membrane lipids.

The effects of pharmacological inhibition of glycolysis or ATP synthase on ΔΨm, ATP production and oxygen consumption revealed that the two cell lines differentially respond to brief treatments with metabolic inhibitors. Subsequent to the blocking of glycolysis, HepG2 cells were able to activate silent mitochondria, while in JHH-6 an optimization of OXPHOS coupling and phosphorylating respiration [ATP synthesis by the PS] occurred without any improvement of the ETS capacity. Moreover, we found that ΔΨm collapsed when JHH-6 cells were treated with oligomycin, suggesting that proton pumping linked to the

hydrolysis of ATP by ATP synthase, working in its reverse mode, contributed to the maintenance of $\Delta\Psi m$ in these cells at the expense of glycolytic ATP production. Thus, we reveal a relationship between the impairment of the OXPHOS system and the reverse functioning of ATP synthase, although this is probably only one way by which the reverse mode of the enzyme is driven. Notably, the reverse mechanism of ATP synthase has already been documented as an important pathogenic mechanism in diseases in which mitochondrial respiration is compromised (Harris and Das 1991), although this mechanism is not yet fully understood [for a review see (Chinopoulos and Adam-Vizi 2010)]. For example, the mitochondrion as an ATP consumer has been documented in cells derived from patients (with clinical encephalopathy and lactic acidosis) carrying a mitochondrial DNA mutation affecting proton pumping at complex I (McKenzie et al. 2007). Nevertheless, to our knowledge in cancer cells only few reports exist on this topic; in particular, ATP synthase has been found to function in the reverse mode in 143B human osteosarcoma cells, where it was linked to the overexpression of the adenine nucleotide translocator isoform 2 (ANT2), which operates the ATP/ADP exchange in reverse, thereby importing glycolytic ATP into mitochondria (Chevrollier et al. 2005). ANT2 is highly expressed in proliferating cells, and its induction in cancer cells is known to be directly associated with glycolytic metabolism and carcinogenesis (Chevrollier et al. 2005). It plays a critical role in conveying ATP into the mitochondrial matrix at a sufficient rate for the ATPase to hydrolyze (Chinopoulos et al. 2009), even if very few studies in the literature have addressed this function of ANT2 (Chevrollier et al. 2010). A physical link between ATP synthase and ANT has been demonstrated by Pedersen and co-workers, which together may form a so-called ATP synthasome (Chen et al. 2004). According to the Pedersen mechanism, hexokinase isoform 2, the predominant over-expressed isoform in malignant tumours, is strategically bound to the external side of the mitochondrial outer membrane and it is not regulated by its product glucose 6-phosphate; moreover, it gains preferential access to mitochondria-generated ATP through a structural/functional interaction with the ATP synthasome (Mathupala et al. 2010).

The most important finding of the present study, however, is the connection revealed between the up-regulation of the expression of ATP synthase natural inhibitor IF1 and a better yield of IF1 productive association with the complex in more proliferating/less differentiated cell line. Indeed, IF1 is known to inhibit ATPase activity in response to the reversal of ATP synthase activity (Campanella et al. 2009; Di Pancrazio et al. 2004; Lippe et al. 2009; Penna et al. 2004). Nevertheless, we know almost nothing about the relative expression levels of IF1 in different tissues and cell types, about the physiological impact of differing IF1 expression levels, or the mechanism that regulates its expression. Interesting speculation was prompted about the role of IF1 in tumour metabolism by pioneer reports (Chernyak et al. 1991; Bravo et al. 2004), but the results presented urge for more definitive studies to be performed to firmly establish such a role. A recent report by Cuevza and colleagues, based on analysis in paired normal and tumour biopsies, shows that in some human tissues carcinogenesis promotes IF1 over-expression and suggests that the participation of IF1 in oncogenesis may act as an additional molecular switch used by cancer cells to trigger the induction of aerobic glycolysis, i.e., their Warburg phonotype (Sanchez-Cenizo et al. 2010). Nevertheless, the biochemical mechanism by which IF1 elicits such effect is still unclear and it may depend upon the bioenergetic state of mitochondria. In the present study, we demonstrate a higher expression level of IF1 in undifferentiated JHH-6 compared with HepG2, which retain characteristics of differentiating cells. This overexpression corresponds to a higher association of IF1 with the ATP synthase complex and hence enhanced inhibition. We conclude that the ATP synthase activity in JHH-6 is more tightly regulated by IF1, in accordance with the large extent of reverse ATP synthase functioning in these cells; this may represent a mechanism by which ATP depletion is controlled and the $\Delta\Psi m$ sustained contributing to a more proliferating tumour phenotype. Our results, while confirming the over-expression of IF1 in cancer cells, are the first to document a link between IF1 expression level and amount actually bound to ATP synthase, and to point to an inverse relationship with the cell differentiation status and aggressiveness. These findings will facilitate the future design of therapies targeting the bioenergetic features of hepatocellular carcinomas.

**Funding** This work was supported by the Italian Ministero dell'Università e della Ricerca Scientifica (MIUR) through a Progetto di Rilevanza Nazionale (PRIN) grant

## References

Arismendi-Morillo G (2009) Int J Biochem Cell Biol 41:2062–2068
Bellance N, Benard G, Furt F, Begueret H, Smolkova K, Passerieux E, Delage JP, Baste JM, Moreau P, Rossignol R (2009) Int J Biochem Cell Biol 41:2566–2577
Bravo C, Minauro-Sanmiguel F, Morales-Rios E, Rodriguez-Zavala JS, Garcia JJ (2004) J Bioenerg Biomembr 36:257–264
Campanella M, Parker N, Tan CH, Hall AM, Duchen MR (2009) Trends Biochem Sci 34:343–350
Chen C, Ko Y, Delannoy M, Ludtke SJ, Chiu W, Pedersen PL (2004) J Biol Chem 279:31761–31768
Chernyak BV, Dukhovich VF, Khodjaev E (1991) Arch Biochem Biophys 286:604–609
Chevrollier A, Loiseau D, Chabi B, Renier G, Douay O, Malthiery Y, Stepien G (2005) J Bioenerg Biomembr 37:307–316

Chevrollier A, Loiseau D, Stepien G, Reynier P (2010) Biochim Biophys Acta. (in press)
Chinopoulos C, Adam-Vizi V (2010) Biochim Biophys Acta 1802:221–227
Chinopoulos C, Vajda S, Csanady L, Mandi M, Mathe K, Adam-Vizi V (2009) Biophys J 96:2490–2504
Comelli M, Lippe G, Mavelli I (1994) FEBS Lett 352:71–75
Contessi S, Comelli M, Cmet S, Lippe G, Mavelli I (2007) J Bioenerg Biomembr 39:291–300
Cossarizza A, Salvioli S (2001) Current protocols in cytometry Chapter 9: unit 9.14
Cuezva JM, Krajewska M, de Heredia ML, Krajewski S, Santamaria G, Kim H, Zapata JM, Marusawa H, Chamorro M, Reed JC (2002) Cancer Res 62:6674–6681
Cuezva JM, Ortega AD, Willers I, Sánchez-Cenizo L, Aldea M, Sánchez-Aragó M (2009) Biochim Biophys Acta 1792:1145–1158
DeBerardinis RJ, Lum JJ, Hatzivassiliou G, Thompson CB (2008) Cell Metab 7:11–20
Di Pancrazio F, Mavelli I, Isola M, Losano G, Pagliaro P, Harris DA, Lippe G (2004) Biochim Biophys Acta 1659:52–62
Di Pietro A, Penin F, Julliard JH, Godinot C, Gautheron DC (1988) Biochem Biophys Res Commun 152:1319–1325
Frezza C, Gottlieb E (2009) Semin Cancer Biol 19:4–11
Giorgio V, Bisetto E, Soriano ME, Dabbeni-Sala F, Basso E, Petronilli V, Forte MA, Bernardi P, Lippe G (2009) J Biol Chem 284:33982–33988
Gnaiger E (2008) Mitochondrial dysfunction in drug-induced toxicity: 327–352
Grassi G, Scaggiante B, Farra R, Dapas B, Agostini F, Baiz D, Rosso N, Tiribelli C (2007) Biochimie 89:1544–1552
Green DW, Grover GJ (2000) Biochim Biophys Acta 1458:343–355
Grover GJ, Atwal KS, Sleph PG, Wang FL, Monshizadegan H, Monticello T, Green DW (2004) Am J Physiol Heart Circ Physiol 287:H1747–H1755
Hanahan D, Weinberg RA (2000) Cell 100:57–70
Harris DA, Das AM (1991) Biochem J 280:561–573
Hernlund E, Hjerpe E, Avall-Lundqvist E, Shoshan M (2009) Mol Cancer Ther 8:1916–1923
Ihrlund LS, Hernlund E, Khan O, Shoshan MC (2008) Mol Oncol 2:94–101
Ishikawa K, Takenaga K, Akimoto M, Koshikawa N, Yamaguchi A, Imanishi H, Nakada K, Honma Y, Hayashi J (2008) Science 320:661–664
Kim HK, Park WS, Kang SH, Warda M, Kim N, Ko JH, Ael B, Han J (2007) Am J Physiol Cell Physiol 293:C761–C771
Kroemer G, Pouyssegur J (2008) Cancer Cell 13:472–482
Kurtoglu M, Lampidis TJ (2009) Mol Nutr Food Res 53:68–75
Lippe G, Bisetto E, Comelli M, Contessi S, Di Pancrazio F, Mavelli I (2009) J Bioenerg Biomembr 41:151–157
Loiseau D, Morvan D, Chevrollier A, Demidem A, Douay O, Reynier P, Stepien G (2009) Mol Carcinog 48:733–741
López-Ríos F, Sánchez-Aragó M, García E, Ortega AD, Berrendero JR, Pozo-Rodríguez F, López-Encuentra A, Ballestín C, Cuezva JM (2007) Cancer Res 67:9013–9017
Marroquin LD, Hynes J, Dykens JA, Jamieson JD, Will Y (2007) Toxicol Sci 97:539–547
Mathupala SP, Ko YH, Pedersen PL (2010) Biochim Biophys Acta 1797:1225–1230
McKenzie M, Liolitsa D, Akinshina N, Campanella M, Sisodiya S, Hargreaves I, Nirmalananthan N, Sweeney MG, Abou-Sleiman PM, Wood NW, Hanna MG, Duchen MR (2007) J Biol Chem 282:36845–36852
Modica-Napolitano JS, Aprille JR (2001) Adv Drug Deliv Rev 49:63–70
Moreno-Sanchez R, Rodriguez-Enriquez S, Marin-Hernandez A, Saavedra E (2007) FEBS J 274:1393–1418
Oliva CR, Nozell SE, Diers A, McClugage SG, Sarkaria JN, Markert JM, Darley-Usmar VM, Bailey SM, Gillespie GY, Landar A, Griguer CE (2010) J Biol Chem 285:39759–39767
Paumard P, Vaillier J, Coulary B, Schaeffer J, Soubannier V, Mueller DM, Brethes D, di Rago JP, Velours J (2002) EMBO J 21:221–230
Penna C, Pagliaro P, Rastaldo R, Di Pancrazio F, Lippe G, Gattullo D, Mancardi D, Samaja M, Losano G, Mavelli I (2004) Am J Physiol 287:H2192–H2200
Putignani L, Raffa S, Pescosolido R, Aimati L, Signore F, Torrisi MR, Grammatico P (2008) Breast Cancer Res Treat 110:439–452
Rouslin W, Broge CW (1996) J Biol Chem 271:23638–23641
Sanchez-Arago M, Chamorro M, Cuezva JM (2010) Carcinogenesis 31:567–576
Sanchez-Cenizo L, Formentini L, Aldea M, Ortega AD, Garcia-Huerta P, Sanchez-Arago M, Cuezva JM (2010) J Biol Chem 285:25308–25313
Shaw RJ (2006) Curr Opin Cell Biol 18:598–608
Simonnet H, Alazard N, Pfeiffer K, Gallou C, Beroud C, Demont J, Bouvier R, Schagger H, Godinot C (2002) Carcinogenesis 23:759–768
Solaini G, Sgarbi G, Baracca A (2010) Biochim Biophys Acta (in press)
Srere PA (1969) Methods Enzymol 13:3–5
Warburg O (1956) Science 123:309–314
Willers IM, Cuezva JM (2010) Biochim Biophys Acta (in press)
Zu XL, Guppy M (2004) Biochem Biophys Res Commun 313:459–465